

**Molecular Dynamics Insights into the Interactions of a Potential Neurotherapeutic Peptide
with Model Liposomes**

SUPPORTING INFORMATION

Gulsah Gul^{1,*}

¹Department of Chemical and Biological Engineering, Koç University, İstanbul, Turkey,

*gugul@ku.edu.tr

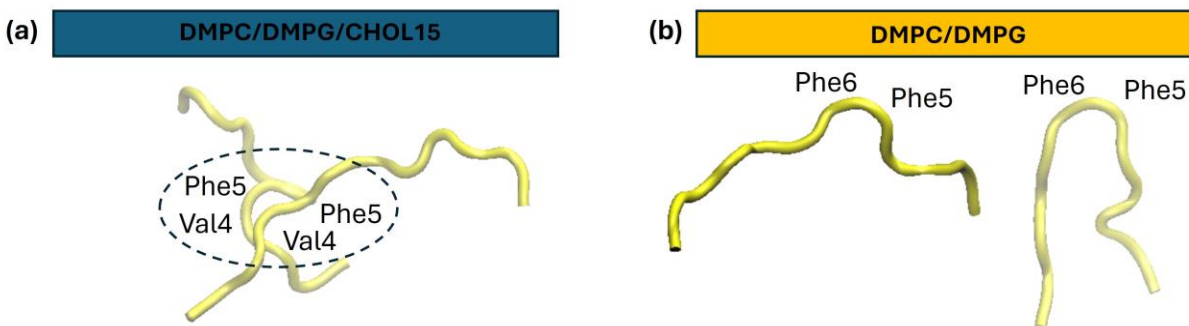


Figure S1. Representative conformations of aggregated peptides in DMPC/DMPG/CHOL15 membrane highlighting interacting residues **(a)** and peptide insertion in DMPC/DMPG membrane from two independent trials **(b)**.

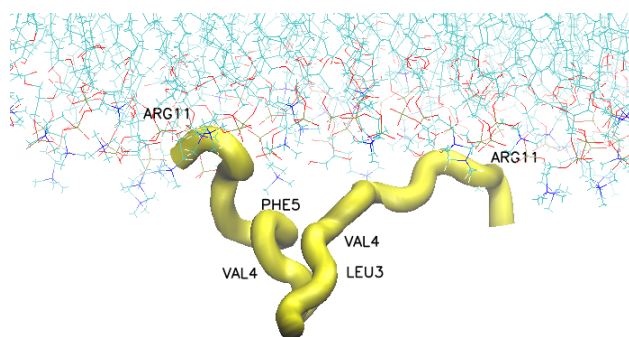


Figure S2. Peptide–lipid association for the peptide dimer in DMPC/DMPG/CHOL15 membrane. C-terminal Arg residues interact with the lipid headgroups, while Leu3, Val4 and Phe5 participate in the dimer interface.

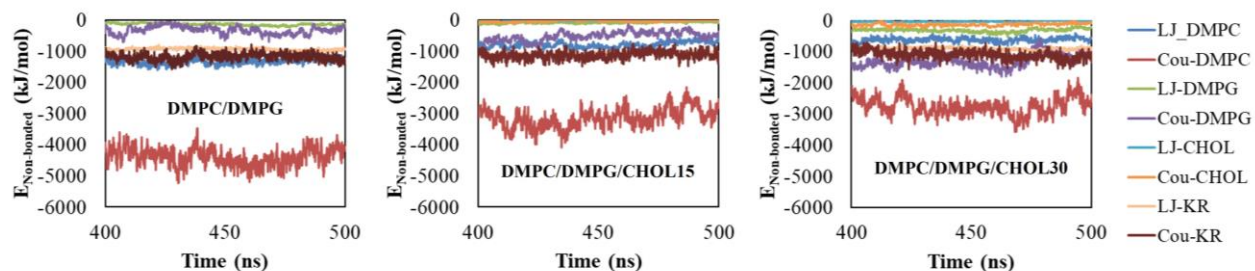


Figure S3. Short-ranged non-bonded interaction energies between peptides (KR), and between peptides and lipid components (DMPC, DMPG, CHOL) over time. Here, LJ stands for Lennard Jones interactions while Cou represents Coulombic electrostatics.

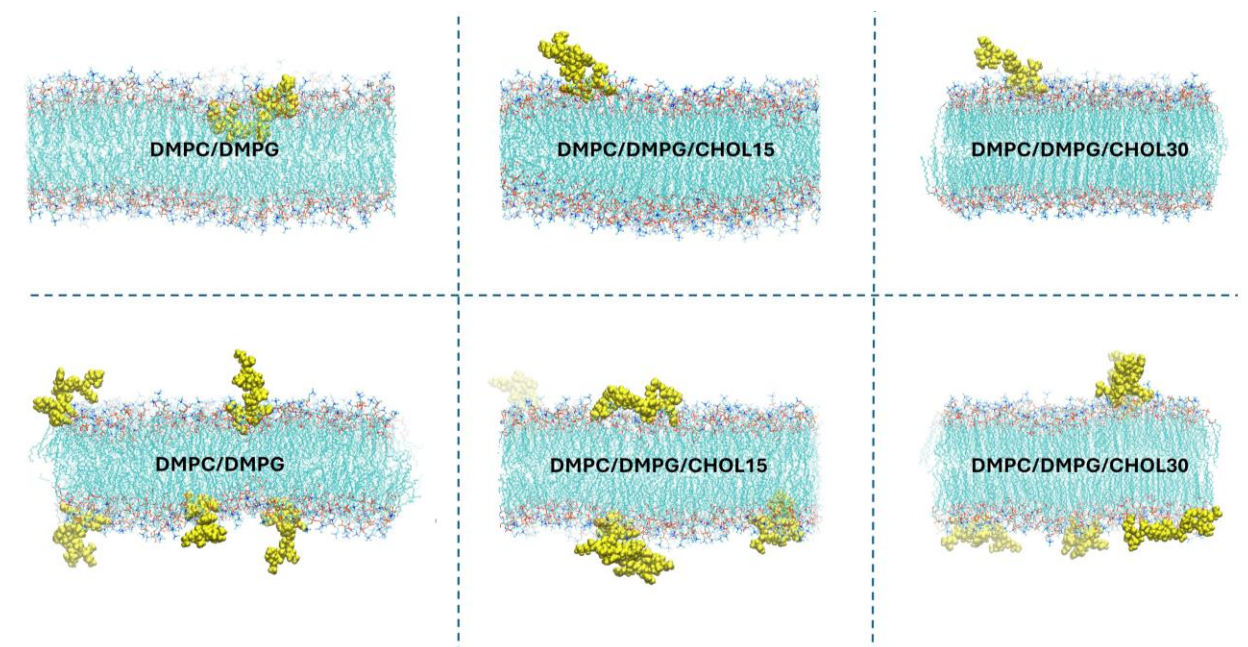


Figure S4. Distribution of KR peptides across DMPC/DMPG membranes with varying cholesterol content, taken from the second independent trial. The upper panel shows systems containing a single KR peptide, while the lower panel shows systems with five KR peptides. Here, peptide molecules are represented by yellow van der Waals spheres.

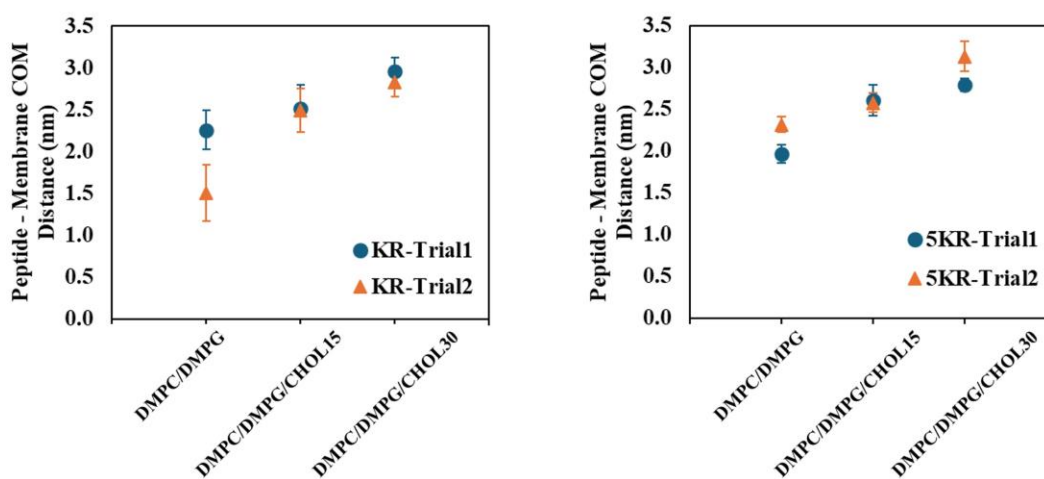


Figure S5. Average center-of-mass (COM) distance between peptides and DMPC/DMPG membranes with varying cholesterol (CHOL) concentrations, calculated over the last 100 ns of the simulations. The left panel shows systems containing a single KR peptide, whereas the right panel shows systems containing five KR peptides.

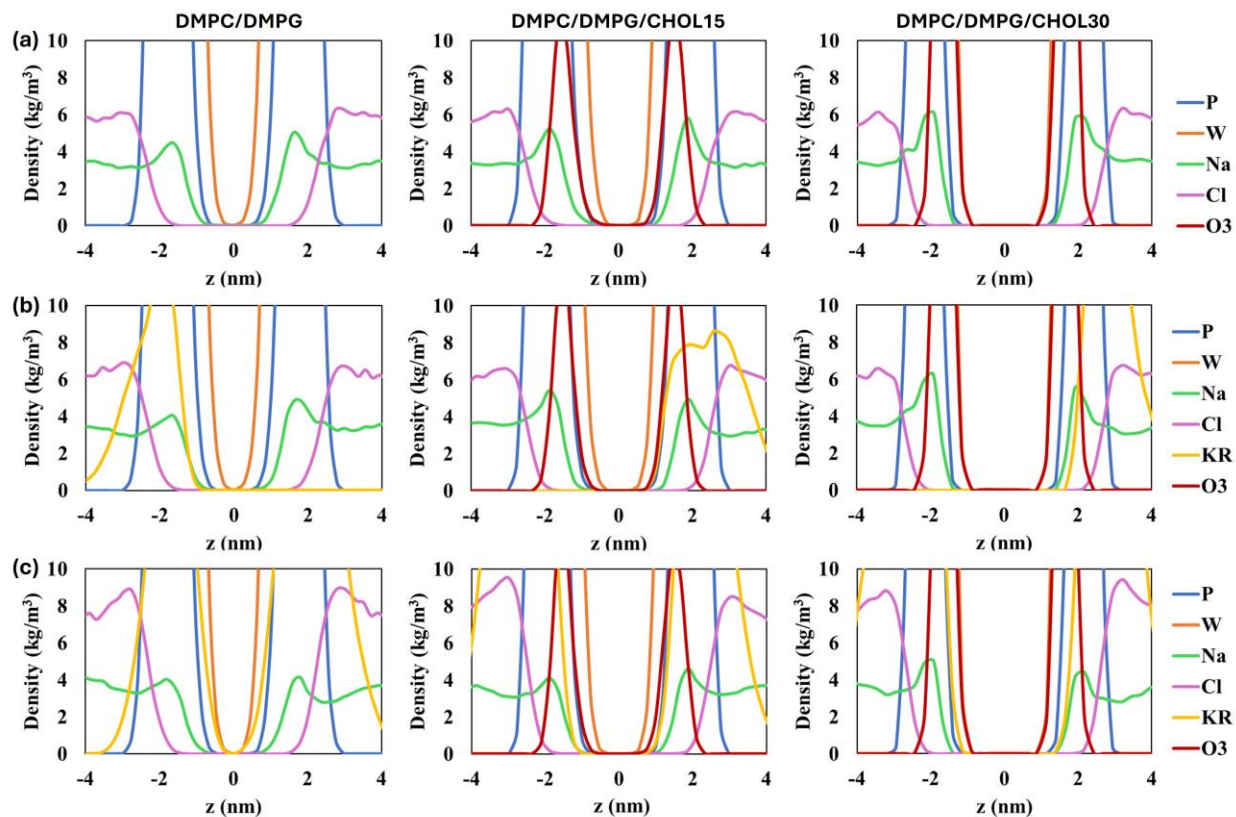


Figure S6. Magnified density distributions of phosphorus (P), water (W), sodium (Na), chloride (Cl), peptide (KR), and cholesterol oxygen (O3) in DMPC/DMPG membranes with varying cholesterol levels, relative to the membrane center ($z = 0$). Profiles are shown for bare membranes **(a)**, membranes containing a single KR peptide **(b)**, and membranes containing five KR peptides **(c)**.

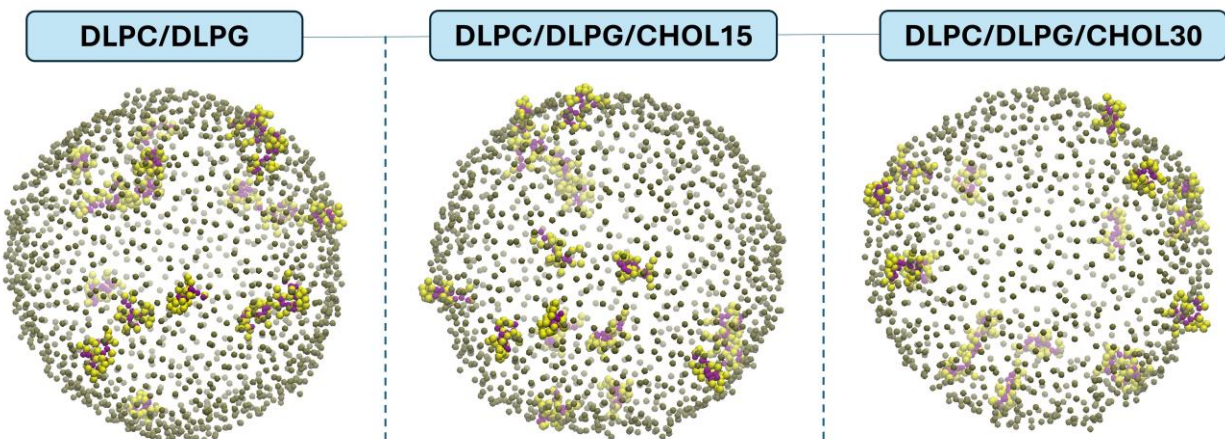


Figure S7. Peptide distribution in the lower leaflet of DLPC/DLPG liposomes containing 0, 15, and 30% CHOL (left to right) at 2 μ s. For clarity, only the inner-leaflet PO₄ beads and peptides are shown, rendered as tan and yellow van der Waals spheres, respectively.

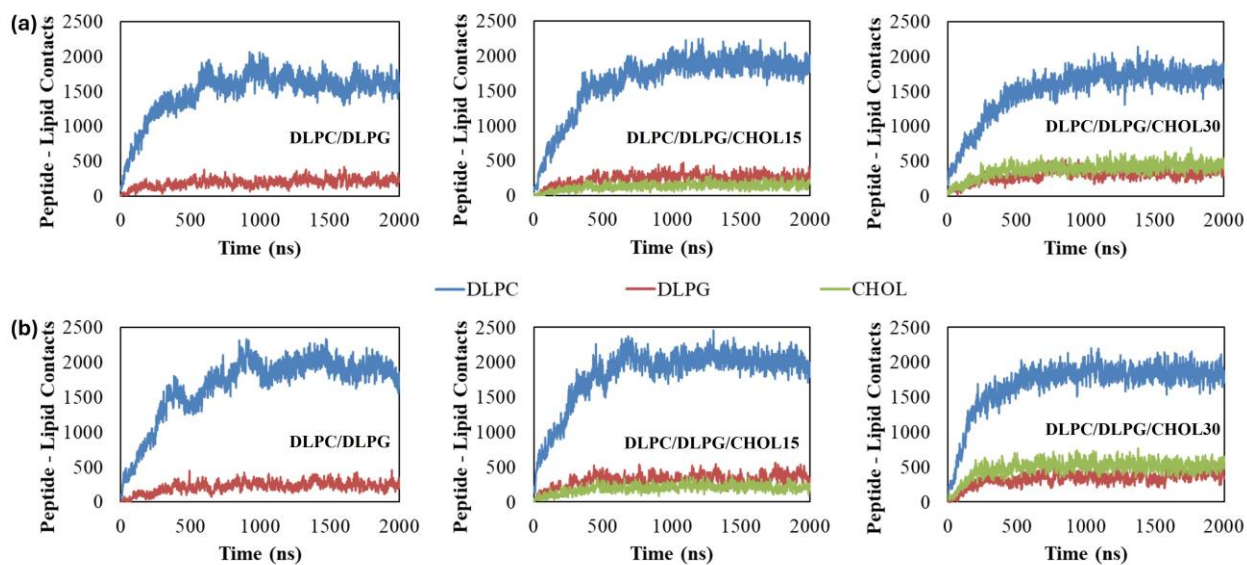


Figure S8. The time evolution of peptide - lipid contacts in DLPC/DLPG bilayers containing 0, 15, and 30% CHOL (left to right). The upper panel **(a)** corresponds to the external initial placement of peptides, whereas the lower panel **(b)** corresponds to their initial partial embedment.

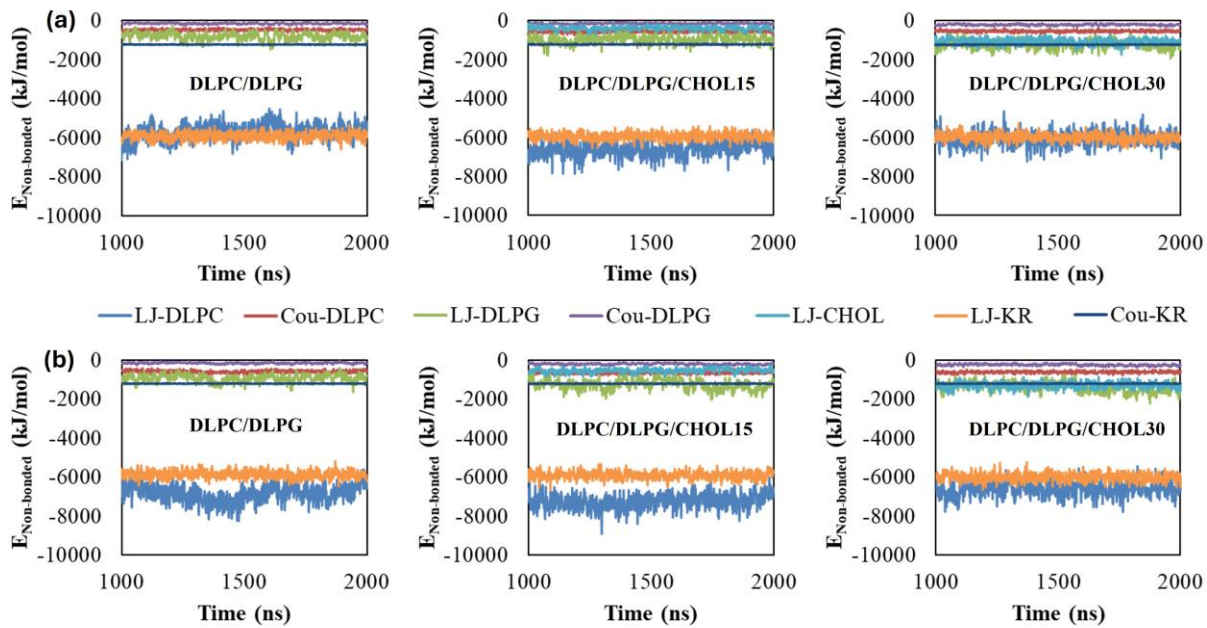


Figure S9. Short-ranged non-bonded interaction energies between peptides (KR), and between peptides and lipid components (DMPC, DMPG, CHOL) over time. The upper panel **(a)** corresponds to the external initial placement of peptides, whereas the lower panel **(b)** corresponds to their initial partial embedment.

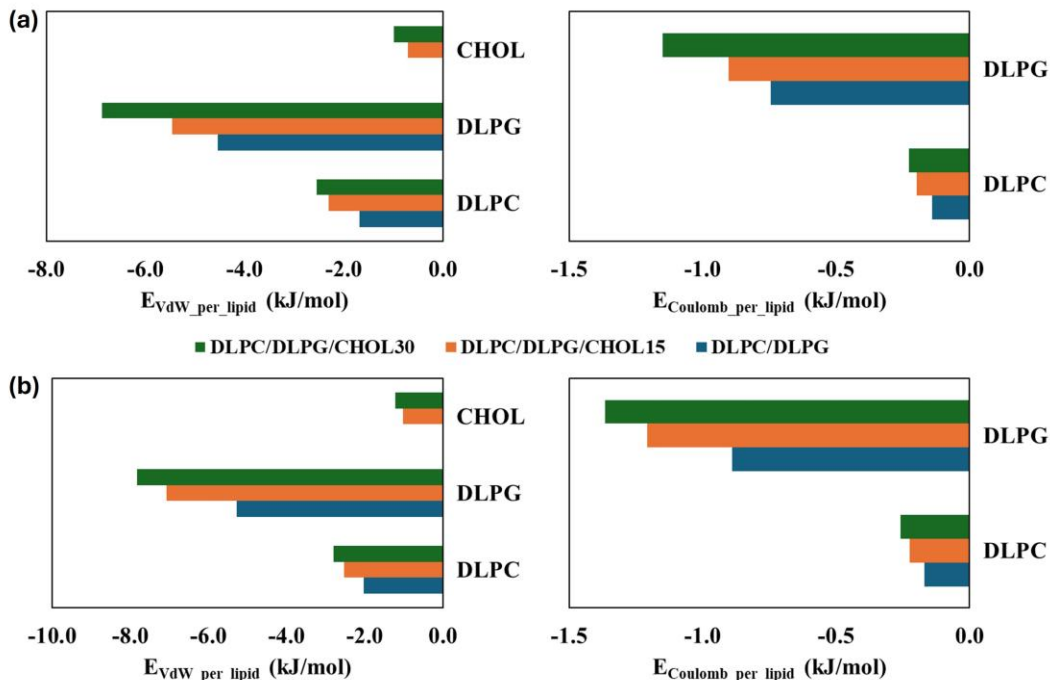


Figure S10. Average van der Waals (left) and coulombic (right) interaction energies-per-lipid between peptides and each lipid type in DLPC/DLPG liposomes with varying CHOL levels. The upper panel (a) corresponds to the external initial placement of peptides, whereas the lower panel (b) corresponds to their initial partial embedment.

Table S1. MM-PBSA binding free energies of the single KR peptide with pure DMPC and DMPG lipid membranes, including van der Waals (VDWAALS) and electrostatics (EEL) contributions. The Poisson–Boltzmann equation was solved using the geometric multigrid approach ($solvopt = 2$) with linear PB ($ipb = 1$) and periodic boundary conditions ($bcopt = 10$) to minimize unphysical edge effects. The parameter $eneopt$ was set to 1 as the charge-view method ($eneopt = 2$) is not supported for protein-membrane systems; consequently, the EEL term includes both Coulombic and reaction-field (EPB) energies.

	$\Delta E_{VDWAALS}$ (kJ/mol)	ΔE_{EEL} (kJ/mol)	ΔG_{solv} (kJ/mol)	$\Delta G_{binding}$ (kJ/mol)
DMPC	-50.2 ± 9.5	-79.9 ± 34.3	-10.0 ± 0.8	-140.1 ± 29.1
DMPG	-91.9 ± 9.4	-286.4 ± 34.8	-13.8 ± 0.6	-392.1 ± 35.2